





RESEARCH ARTICLE

WILEY

Shooting for abundance: Comparing integrated multi-sampling models for camera trap and hair trap data

Mehnaz Jahid¹ | Holly N. Steeves²  | Jason T. Fisher³  | Simon J. Bonner²  |
Saman Muthukumarana⁴  | Laura L. E. Cowen¹ 

¹Department of Mathematics and Statistics, University of Victoria, Victoria, British Columbia, Canada

²Department of Statistics and Actuarial Sciences, University of Western Ontario, London, Ontario, Canada

³School of Environmental Studies, University of Victoria, Victoria, British Columbia, Canada

⁴Department of Statistics, University of Manitoba, Winnipeg, Manitoba, Canada

Correspondence

Mehnaz Jahid, Department of Mathematics and Statistics, University of Victoria, Victoria, BC V8W 2Y2, Canada.
Email: mehnazjahid@uvic.ca

Funding information

Alberta Innovates-Technology Futures and Alberta Environment and Parks (AEP); Canadian Statistical Sciences Institute

Abstract

Abundance estimation is a vital goal in wildlife monitoring. Camera-traps are a tool to survey wildlife populations noninvasively and can be used for abundance estimation if individuals are identifiable. However, for species without individual identification characteristics, camera-trap surveys have often been combined with some other survey method such as capture-recapture (CR, using traditional tags or DNA through hair snags or scat) to inform an integrated model. We discuss and apply two integrated models involving presence-absence data from camera traps and CR data from hair traps to compare bias and precision to estimate the population density of grizzly bears of the central Rocky Mountains of Alberta, Canada. Unlike many other studies, we found that integrating presence-absence data with CR data does not improve the precision of the density estimates. The possible reasons for such results are discussed in detail.

KEYWORDS

abundance, Bayesian, camera trap, data integration, grizzly bear, occupancy

1 | INTRODUCTION

Wildlife monitoring programs provide valuable information on the state of populations and how they are affected by human activity, including landscape management and harvesting decisions (Yoccoz et al., 2001). This science-based information may then be used to plan efficient ecosystem activities without which threatened species may face extinction (Huettmann, 2005; White, 2001). Different methods are available for monitoring populations of animals and the appropriate method may be selected according to the study objectives, available resources, feasibility of different field techniques, and behavior of the species of interest (Witmer, 2005). An important objective in these programs is monitoring species abundance and density (Devarajan et al., 2020), which helps track changes in population abundance over space and time (Gibbs, 2000).

Broadly speaking, methods of monitoring animal populations may be classified according to whether or not they allow for individuals within the population to be identified and followed over time. If individuals are identifiable then capture-recapture (CR), or related, methods may be applied to make inference about the individual demographic processes—recruitment, survival, and movement—that lead to changes in the population over time (Chao, 1987; Pollock, 2000). Extensions of the standard CR models incorporating covariates may also be fit to identify the effects

that different individual characteristics and environmental factors have on population processes (see, e.g., Lebreton et al., 1992; Schofield & Barker, 2011; Schwarz & Arnason, 1996). This information may then be used to study the dynamics of the population as a whole and, for example, to estimate the size of a population or how the abundance or density of a species changes over time and/or space.

If individuals cannot be identified then it may only be possible to model the presence/absence of a species, for example, with site occupancy models (MacKenzie et al., 2002, 2017). Recently, it has become more common for studies to combine different field techniques, with one method providing information on occupancy at sites across a broad study area, while the second method provides detailed information on the capture histories of a small number of identified individuals (see, e.g., Besbeas et al., 2002; Zipkin & Saunders, 2018). Various statistical models to integrate these two forms of data have recently been developed; however, their accuracy and precision have not been widely explored.

As an example of the integrated modeling approach, we consider data from a study of grizzly bears (*Ursus arctos*) conducted in the Rocky Mountains of Alberta, Canada, in 2012 (Fisher et al., 2016). Several detection sites were installed over a large area and each site contained both a hair snare, consisting of barbed wire against which the bears would rub, and a passive camera trap. Further details of the sampling protocol are provided in Section 3.

The advancement of PCR amplification of DNA samples, as well as advanced DNA analysis (such as nuclear microsatellites and SNPs), have allowed DNA-based sampling of wildlife populations to proliferate, and hair traps are the most common method of collecting DNA for mammals (Kendall & McKelvey, 2008). The greatest advantage of DNA-based sampling is the comparative wealth of information that DNA can provide. DNA not only allows for individual identification, but also provides information on parentage, relatedness, and heterozygosity, all in a spatial context from which inferences on complex aspects of the population can be made (Balkenhol et al., 2015). A primary disadvantage is that genetic analysis is expensive and the cost increases with the number of samples collected (not necessarily with the number of traps deployed). This means that only a fraction of the samples collected may be identified in some cases, with candidate samples subsetting randomly or by visual inspection. Moreover, due to cost researchers may also have to restrict their analysis to a small number of target species, which may prevent inferences about multiple populations and interactions in the context of sympatric wildlife communities. Another disadvantage comes from variable detectability. False absences often occur with hair traps because animals fail to engage with the hair trap, the device does not trap a hair with a follicle (the part of the hair containing DNA), the DNA degrades due to heat and moisture while in the trap, or DNA samples from multiple animals become mixed. Moreover, some types of hair traps become depleted once they have collected a sample and cannot detect more individuals, and others rely on bait that can decay, reducing detection rates over time.

In comparison, camera traps have become increasingly common, particularly for studying large mammals (Davis et al., 2018; Karanth, 1995; Palencia et al., 2019). Camera traps are generally triggered by infrared sensing of body-heat as animals move through the field of vision. The key advantage of camera traps is that they can be deployed for long periods of time without intervention by the researchers. Developments in battery technology mean that cameras may now be active in the field for several consecutive months, collecting data on an almost continuous basis. Barring camera failure or poor placement, this provides for more reliable detection. Previous comparisons of the two types of monitoring showed that camera traps can produce markedly more detections of large mammals than hair snares located at the same sites (Fisher & Bradbury, 2014; Fisher et al., 2016). However, the disadvantage of camera traps for monitoring most mammal species (including grizzly bears), is that the animals do not possess unique markings and cannot be individually identified. Estimates of abundance or density then rely on assumptions about individual behavior that cannot be tested and may not accurately reflect the true population state. As an example, Burgar et al. (2018) showed striking differences in estimated fisher (*Pekania pennanti*) populations based on unmarked, camera-only density estimates versus marked DNA-based estimates.

With increasing interest in using camera traps to study species that are not individually identifiable, and recognizing shortfalls induced by lack of individual identification, there is an opportunity to make use of methods that combine multiple population surveys into an integrated model to estimate abundance (Besbeas et al., 2002). Integrated modeling allows for the joint analysis of several datasets with inference based on the joint likelihood. Traditionally, integrated population models (IPMs) have been used to describe the modeling of population count data with some form of demographic data in the early papers of Besbeas et al. (2002, 2005) and Schaub and Abadi (2011); however, more recent definitions of IPMs expand the population data to include census and occupancy (Zipkin & Saunders, 2018).

Integrating sampling techniques holds great promise to overcome disadvantages while capitalizing on advantages of both methods, providing for more reliable sampling and hence more robust inferences (Campbell et al., 2008; Fisher & Bradbury, 2014; Magoun et al., 2011). Our interest is to investigate methods of combining data from camera traps with data from DNA hair traps to estimate abundance or density. Specifically, we compare grizzly bear density estimates with

two modeling frameworks. First, Blanc et al. (2014) combine camera trap data with DNA from scat data and develop a model to estimate abundance using an occupancy and CR framework. Second, Tourani et al. (2020) use camera trap data with spatially sampled DNA data to develop a combined occupancy and spatial CR model to estimate abundance. Using the data from the Alberta grizzly bear study we compare estimates of abundance based on six different models:

1. Individual heterogeneity model in the capture recapture framework using the identified detection data from hair trap survey, Model CR (Otis et al., 1978).
2. Combined model described in Blanc et al. (2014) using both identified detection data from the hair trap survey and unidentified detection data from the camera trap survey, Model CR-O.
3. Spatially explicit capture-recapture (SECR) model using identified detection data from the hair traps, Model SECR (Efford, 2004).
4. Model 3 in Tourani et al. (2020) which integrates both identified detection data from the hair trap and unidentified detection data from the camera trap survey, Model SECR-O.
5. Model SECR including sex as a covariate, Model SECR(sex).
6. Model SECR-O including sex as a covariate, Model SECR(sex)-O.

We begin by reviewing the models in detail and then compare the models through the grizzly bear case study.

2 | METHODS

Sollmann (2018) provides a thorough review of state-of-the-art camera-trap data analysis methods including both occupancy and spatial CR analyses. We add to this review by studying methods that integrate occupancy data when individuals cannot be identified from camera traps with CR data of individuals marked through some other means. We begin by reviewing the methods of closed CR and spatial CR on their own and then review models that integrate these methods with models for unidentified camera trap presence-absence data.

2.1 | CR (closed model M_h)

CR methods have been widely used for estimating parameters such as population size, survival rate, recruitment rate, and migration rate (Seber, 2002). Closed-population CR models assume the population is closed to births/deaths and immigration/emigration throughout the study period. The traditional CR sampling scheme is comprised of repeated occasions on which animals are sampled from the population, marked with unique tags, and released back into the population. Assuming that all individuals have the same probability of inclusion in each sample, the number of unmarked (newly captured) and marked (recaptured) individuals in each sample is modeled to obtain information about the probability of capture and the size of the population. To apply this type of closed-population CR modeling to camera trap data for population size estimation, individual identification from the photographs is required (Foster & Harmsen, 2012). This is possible for some species of large mammals that have unique patterning. For instance, tigers (*Panthera tigris*), leopards (*Panthera pardus*), and jaguars (*Panthera onca*) have unique pelt patterns from which individuals can be identified. For some other species which do not have unique pelage markings, individual identification is not possible without marks or tags. In such cases, some researchers capture and uniquely mark individuals, releasing them into the population in a typical CR routine, then use mark-resight models to estimate density (Efford & Hunter, 2018; Rich et al., 2014; Sollmann et al., 2013; Whittington et al., 2018).

To model these closed-population CR data, Otis et al. (1978) introduced a variety of models that allow for all possible combinations of time dependence, behavioral effects, and unexplained random heterogeneity in the capture probabilities. Here we focus on the model incorporating unexplained heterogeneity, typically denoted as model M_h . The assumptions for the M_h model are:

1. The population is both geographically (no immigration or emigration) and demographically (no birth or death) closed during the sampling period.
2. Individuals do not lose their marks and the observers always observe the marks correctly.
3. Each individual in the population has a unique probability of capture that is the same on all sampling occasions.

Following the approach of Schofield and Barker (2014) we perform inference in the Bayesian framework and consider the model including the abundance, N , explicitly in the likelihood function rather than as a derived parameter. In this model, the i th individual has its own capture probability p_i that is constant over all sampling occasions. Otis et al. (1978) consider p_1, \dots, p_n to be a random sample of size n from a distribution F_p defined between 0 and 1 (e.g., the beta distribution).

To describe this mathematically, let X be the $N \times J$ matrix of capture histories for the J sampling occasions. Here, x_{ij} is 1 when individual i is observed at sampling occasion j and 0 otherwise. The specific model of heterogeneity we consider assumes that $\text{logit}(p_i)$, $i = 1, \dots, N$, are independent and normally distributed with mean μ_p and variance τ_η . The complete data likelihood is

$$[X, p|N, \mu_p, \tau_\eta] = \frac{N!}{\sum_h Z_h!} \prod_{i=1}^N \prod_{j=1}^J p_i^{x_{ij}} (1 - p_i)^{1-x_{ij}} \prod_{i=1}^N \phi\left(\frac{\text{logit}(p_i) - \mu_p}{\sqrt{\tau_\eta}}\right), \quad (1)$$

where Z_h denotes the number of individuals observed with capture history h and $\phi(\cdot)$ is the density of a standard normal distribution. Note that the complete data likelihood is constructed as if the number of individuals never captured, $N - n$, and the true capture probability of each individual, p_1, \dots, p_N , were known. The observed likelihood is then computed by integrating/summing across these values.

2.2 | Spatially explicit capture-recapture

If multiple traps are deployed in an area to capture individuals then the simple CR framework ignores an important source of information that is crucial in abundance estimation: the trapping locations. Efford (2004) developed the framework of spatially explicit CR (SECR) to address this issue and to make use of the trapping locations to estimate wildlife population density (Borchers & Efford, 2008; Efford et al., 2009; Royle et al., 2009; Royle & Young, 2008). Density, D , is estimated by dividing the estimated population size, \hat{N} , by the size of the area occupied by the species, A : $\hat{D} = \hat{N}/A$ (Efford et al., 2009).

The general assumptions of this method are:

1. The population is closed.
2. Each individual has a different activity center (home range center) that is chosen according to some distribution over the study area.
3. Activity centers are fixed during the survey time.
4. The probability that an individual is captured at a specific trap on each occasion declines as the distance from the trap location to the activity center increases.
5. Each of the captures are independent events.

True closure can only be assumed if there is a defined geographic area which is occupied by the species (e.g., an island). Closure is violated to some degree when the species move without a fixed limit beyond the trapping area (Efford et al., 2009). Capture probability is calculated through some function of the Euclidean distance of home range center and trap locations. Efford et al. (2009, p. 256) defined density as “the intensity of a spatial point process for the home range centers.”

To run this analysis, the Cartesian coordinates, for example, longitude (lg) and latitude (lt), of all the trap locations that have been placed in the animal habitat and the capture history of every individual including both capture occasion and location are needed. To explain the model, we first define some notation. Let K be the number of traps placed in the habitat with the k th trap having location (lg_k, lt_k) and J the total number of sampling occasions. Let $\mathbf{h}_i = (h_{i1}, h_{i2})$ denote the coordinates of the home range center of animal i defined across region R and H be the $n \times 2$ matrix of all the home ranges. Further, let

$$\delta_{ikj} = \begin{cases} 1; & \text{if individual } i \text{ is detected at trap } k \text{ on occasion } j, \\ 0; & \text{otherwise} \end{cases}$$

and

$$\delta_{i,j} = \begin{cases} 1; & \text{if } \sum_k \delta_{ikj} > 0, \text{ individual } i \text{ is detected on occasion } j, \\ 0; & \text{otherwise.} \end{cases}$$

In this case, the $K \times J$ matrix with entries δ_{ikj} , denoted Δ_i , represents the capture history for individual i including the trap location information. The J -vector of values $\delta_{i,j}$ represents the capture history ignoring the trap information.

The likelihood of capturing n unique individuals and their capture history can be defined as the product of the marginal distribution of n and conditional distribution of the observed capture histories given that n animals have been captured (Efford et al., 2009). Additionally, by assuming that the capture events are independent, that the marginal distribution of n is defined as a homogeneous Poisson distribution with rate parameter equal to the average density times the mean detection probability, $D \times a$, and that θ is the vector of detection parameters, we obtain the likelihood as follows:

$$L(\theta, D|n, \Delta_1, \dots, \Delta_n) = P(n|D, \theta) \times \prod_{i=1}^n \frac{\int_{\mathbf{R}} P(\Delta_i|\mathbf{h}, \theta) d\mathbf{h}}{\int_{\mathbf{R}} p(\mathbf{h}; \theta) d\mathbf{h}}, \quad (2)$$

where $P(\Delta_i|\mathbf{h}, \theta)$ is the probability of observing capture history Δ_i given that the animal has home range center \mathbf{h} in region R and model parameters θ .

As explained by Efford et al. (2009), the value $a = \int_{\mathbf{R}} p(\mathbf{h}; \theta) d\mathbf{h}$ is the spatial analog of the detection probability and is defined in terms of the probability of capturing an individual at least once. This probability depends on the Cartesian distance between the traps and home range center locations ($d_k(\mathbf{h})$):

$$p(\mathbf{h}; \theta) = 1 - \prod_{j=1}^J \prod_{k=1}^K [1 - p_j(d_k(\mathbf{h}); \theta)],$$

where $p_j(d; \theta)$ is the detection function. The idea of this detection function is very similar to the detection functions of distance sampling (Buckland et al., 2001). The detection function in SECR is generally assumed to be of a known form defined up to the values of two parameters. One, often denoted g_0 , represents the probability of detection if a trap was placed directly at the home range center of an individual. The other parameter, often denoted σ , represents the spatial scale of the distance between the home range centers and trap locations with which the detection probability decreases. Three types of detection probability functions are commonly considered in this context: half-normal detection with parameters g_0 and σ , negative-exponential detection with parameters g_0 and σ , and hazard-rate detection with parameters g_0 , σ , and an additional shape parameter b . For all of these detection functions, the detection probability increases if the home range (σ) decreases and decreases if the distance between the home range center and traps (d) increases.

Generally, we can express the probability of observing the capture history x_i given the home range centers as:

$$P(\Delta_i|\mathbf{h}_i, \theta) = \prod_{j=1}^J \left[\prod_{k=1}^K p_{kj}(\mathbf{h}_i, \theta)^{\delta_{ikj}} \right] [1 - p_j(H, \theta)]^{1-\delta_{i,j}},$$

where $p_{kj}(\mathbf{h}_i, \theta)$ is the probability of detecting an individual with home range center \mathbf{h}_i at the k th trap on the j th occasion and $p_j(H, \theta)$ is the probability of detection at any of the K traps on the j th occasion.

For proximity detectors (detectors which allow the animals to visit the other traps within same occasion and also the traps can capture multiple individuals on the same occasion), p_{kj} can be defined by the detection function:

$$p_{kj}(\mathbf{h}_i) = p_j(d_k(\mathbf{h}_i); \theta).$$

Thus, we can say that the probability that the i th individual with home range center H can be detected at the k th trap on the j th occasion depends on the distance between the k th trap and \mathbf{h}_i .

The exact form of the likelihood can be constructed by substituting these expressions into (2), which, in theory, could be maximized with respect to the parameters to obtain the maximum likelihood estimates. However, since we have no information about the home range centers, we have to numerically integrate them out. To do that, researchers need to

define a habitat area or habitat mask (Efford, 2019; Efford et al., 2009). A habitat mask is the habitat area around the trap locations which is potentially occupied by the species. We place the camera traps on a continuous plane but the actual area we are sampling is not well defined. This is addressed in SECR by defining the habitat mask to be a larger area than the area covered by the camera traps. The probability of detection decreases as the distance from the center of activity increases. That is why, its extent is not critical as long as it is large enough to include the home ranges of all potentially detectable animals. To facilitate computation, we can define the area of integration as grid cells of equal area and list the centers of grid cells as discrete points (Efford, 2019). Then we can use these points to calculate the distance between home range centers and trap locations. While defining the habitat mask, we should exclude any “non-habitat” region from the habitat mask (e.g., large water bodies might not be included in the habitats of large mammals) because including non-habitat in the habitat mask can result in density being underestimated.

2.3 | Data integration

2.3.1 | Combining CR and occupancy data

The first integrated data method we explore combines CR and occupancy data to improve abundance estimates as described in Blanc et al. (2014). Occupancy modeling estimates the percentage of the habitat occupied by a species, accounting for imperfect detection. It applies when the study area can be divided into discrete sites. A site is then defined to be occupied if at least one individual is present during the study period. Occupancy models must account for the possibility of imperfect detection since we cannot know the true proportion of occupied sites as we do not observe all individuals. If animals are detected at a site then it must be occupied. However, animals might not be detected either when a site is occupied but the species is not detected, or if the site is not occupied. The general assumptions of the simplest occupancy models are:

1. Target species are never falsely identified in the survey while they are actually absent.
2. The study site is closed to changes with respect to occupancy during the survey period.
3. The probability of occupancy is equal across all sites.
4. Detection histories observed in each sites are independent of other sites.

Extensions of this model do allow for either the probability of occupancy or the probability of detection to vary so that, for example, the probability of occupancy is site-specific.

Let $Y_{s,j}$ represents whether an individual in site s at time j was observed ($Y_{s,j} = 1$) or not ($Y_{s,j} = 0$). Then,

$$[Y_{s,j} | z_{s,j}] \sim \text{Bernoulli}(z_{s,j} \gamma_{o_s}),$$

where $z_{s,j}$ is a realization of the state variable occupancy and γ_{o_s} is the probability of detecting the species in site s .

The method of Blanc et al. (2014) relies on the fact that knowing the occupancy status partially informs the abundance, as if there is occupancy, there must be at least one individual present (Royle & Nichols, 2003). The goal of this method is to estimate abundance, N , as above, which Blanc et al. (2014) consider as a state variable that follows a Poisson distribution with mean λ . Also, let Z_i be a state variable describing whether or not the i th spatial unit is occupied, which follows a Bernoulli distribution with probability ψ . The method of Blanc et al. (2014) connects λ and ψ by assuming that $Z_i = 1$ if and only if $N > 0$. Note, however, that this assumption mixes the scales of observation—abundance is modeled over the entire area while occupancy is modeled at individual sites. We discuss the possible impacts in Section 4.

Following Blanc et al. (2014), the relationship between λ and ψ is determined by the fact that the probability a site is occupied is equal to the probability that more than one individual is present (i.e., abundance is positive). As stated by Blanc et al. (2014):

$$P(N > 0) = 1 - P(N = 0) = 1 - e^{-\lambda} = P(Z = 1) = \psi. \quad (3)$$

Rearranging this, one can obtain:

$$\lambda = -\log(1 - \psi).$$

The CR model makes use of the complete data likelihood approach proposed in Schofield and Barker (2014) as shown in Equation (1). Assumptions for occupancy and CR M_h should be satisfied for this modeling approach, although Blanc et al. (2014) did not explicitly mention this in the paper.

2.3.2 | Integrated spatial CR method

The second integrated data method we consider is based on Model 3 from Tourani et al. (2020). This is a hierarchical SECR model that integrates data from two independent surveys: one with individual identifications and one without. The model is fit via the data augmentation approach described in Royle et al. (2007) which considers a hypothetical super-population of individuals known to be much larger than the actual population. To fit this model, first M is selected, which is a number much larger than the actual population size, in order to account for imperfect detection. The model considers M individuals then models their inclusion in the population based on latent state variable, ω_i , and inclusion probability Ψ as:

$$\omega_i \sim \text{Bernoulli}(\Psi).$$

The population size can then be found by adding up the individuals included in the population:

$$N = \sum_{i=1}^M \omega_i.$$

We will consider $T = 2$ detector types in our study: hair traps and camera traps, corresponding to J^1 and J^2 detectors, respectively. Using the half normal detection function described in Borchers and Efford (2008), the probability of detecting the i th individual at the k th detector of type t for a single occasion is:

$$p_{ik}^t = p_0^t \times e^{-\frac{(d_{ik}^t)^2}{2\sigma^2}} \times \omega_i,$$

where p_0^t is the magnitude parameter for detector type t (the probability of detecting an individual whose home range center coincides with the detector), σ is the scale parameter which depends on the home range size and is shared between detector types, and d_{ik}^t is the distance between activity center H_i and k th detector of type t .

The probability that an individual is identified when it encounters a detector of type t is denoted by α^t . This may be 0, for detectors that never identify individuals, 1, for detectors that always identify individuals, or something in between. Individually identified detections, y_{ik}^t are then modeled as

$$y_{ik}^t \sim \text{Bernoulli}(p_{ik}^t \cdot \alpha^t),$$

while the presence/absence of at least one unidentified detection at the k th detector of type t is modeled as

$$\dot{y}_k^t \sim \text{Bernoulli}(\dot{p}_k^t),$$

where

$$\dot{p}_k^t = 1 - \prod_{i=1}^M (1 - p_{ik}^t \times (1 - \alpha^t))$$

is the probability of detecting at least one individual that is not identified. Home ranges are assumed to be uniformly distributed across the study region, R :

$$H_i \sim \text{Uniform}(R).$$

Again, Tourani et al. (2020) did not explicitly mention the assumptions of this model; however, we believe that assumptions of SECR should be satisfied for this modeling approach.

3 | CASE STUDY

Grizzly bear (*U. arctos*) distribution was sampled in the central Rocky Mountains of Alberta, Canada, within the Western Cordilleran system (see Figure 1 in Fisher et al. (2016). Topography is rugged, with high peaks over 2500 m, steep-sloped ridges, and valley bottoms. Coniferous forests dominate with some deciduous throughout. The systematic sampling design consisted of 10 km × 10 km grid cells, plotted on a digital landscape coverage in ArcGIS (ArcGis 10.2 (Environmental Systems Research Institute, Inc., Redlands, CA, USA). Within each cell, a fixed sampling site was deployed which remained in place for the season. Locations within each cell were subjectively selected to maximize probability of detection. Some grid cells in which known grizzly bear activity was concentrated were divided into four equal sections, and each of these smaller-scale grid cells was surveyed to better serve management objectives. Exploratory analysis showed detectability did not differ between these cells and the main grid so all sample sites were pooled. A total of 50 sites were surveyed monthly between April (den emergence) and November (den re-entry) in 2012.

3.1 | Species sampling

The researchers used two concurrent methods to sample grizzly bears: noninvasive genetic tagging (NGT) via hair sampling and camera trapping. Hair traps used Gaucho® barbed wire (Bekaert, Brussels, Belgium) wrapped around a tree 2-m up the trunk, lured with ca. 5 mL O’Gorman’s LDC scent lure (O’Gorman’s Co., Montana, USA). Grizzly bears investigating the tree rubbed and left hair samples, also triggering the camera. We collected hair from the traps monthly, using sterile techniques. DNA from hairs was analyzed by Wildlife Genetics International (WGI; Nelson, British Columbia, Canada): DNA was extracted using QIAGEN’s DNEasy^U Tissue Kits (QIAGEN, Hilden, Germany) and identified to species using the G10J microsatellite marker to distinguish black bear from grizzly bear hair samples. Hair samples identified as grizzly bear during the G10J marker stage were then subjected to multi-locus genotyping that followed the established 3-phase process of first pass, error checking, and clean-up (Paetkau, 2003; Paetkau et al., 1995). The seven microsatellites G10J, G1A, G10B, G1D, G10H, G10M, G10P were analyzed, and sex was determined using an amelogenin marker. During the clean-up phase, two additional markers (MU50 and CXX110) were used when necessary to ensure no 1 or 2 mismatch pairs (Paetkau, 2003).

At each station we also deployed one Reconyx^U RM30, PM30, or PC85 infrared-triggered digital camera (Reconyx, Holmen, Wisconsin, USA) 6–10 m from the NGT hair-trap tree (Fisher & Bradbury, 2014; Fisher et al., 2016). Camera data were downloaded monthly in conjunction with hair data collection. Images were analyzed using Timelapse Image Analyzer (Greenberg et al., 2019) and summarized for species presence within 30-day periods; each period constituted a single occasion. Likewise, the hair collection during each 30-day period was considered as a single occasion. This survey period was selected based on grizzly bear movement rates; ensuring more than sufficient time for an individual to explore its home range, encounter a sampler, then move to other samplers, to ensure independence among samplers and sampling occasions. The final data frame was comprised of 50 sites (2012), with 8 repeated monthly visits and 2 methods per site.

3.2 | Model implementation

We used these data to estimate grizzly bear abundance using the six models listed in the introduction and to compare precision of the estimates. We acknowledge that these datasets are not independent which violates the assumption of independence in the integrated models. We discuss this issue further in the Discussion.

We implemented the CR model (model M_h) using a Bayesian approach. We set the total number of augmented individuals to $M = 1000$. We allowed that the capture probability is heterogeneous among all individuals in the population so that the capture probability for individual i is P_i . The logit of P_i is modeled as a mean detection probability (μ_p) with an individual random effect. The distribution for the individual random effect parameter is assumed to be $N(0, \sigma_n^2)$ where $\sigma_n^2 \sim \text{Gamma}(1.5, 37.5)$ and $\mu_p \sim \text{Logistic}(0, 1)$. A discrete uniform prior was used for the abundance parameter, N with values $1/M$.

To apply the integrated model described by Blanc et al. (2014), we used the same model specifications that were used in their study. All the parameter specifications for the CR part of the model were the same as the CR M_h model described previously. The part of the model that deals with occupancy was modeled using a site-dependent occupancy (ψ_s) and site-dependent detection probability parameter (p_{0_s}). ψ_s were modeled using a mean occupancy (μ_ψ) and a site random

effect parameter, $(\beta_s) \sim N(0, \sigma_\beta^2)$. The priors of these parameters are: $\mu_\psi \sim N(0, 5)$ on a log scale and $\sigma_\beta^2 \sim \text{Uniform}(0, 5)$. The logit of the detection probability, p_{0s} , were assumed to be normally distributed with mean μ_p and variance σ_ϵ^2 . The priors of these parameters are: $\mu_p \sim N(0, 10)$ and $\sigma_\epsilon^2 \sim \text{Uniform}(0, 10)$.

To implement the sex-specific SECR model in a Bayesian framework, a mask was defined with a 30 km buffer around the trapping area. We set $M = 1000$ as the total augmented population size. A $\text{Uniform}(0, 1)$ prior was used for the inclusion probability parameter ψ that governed the Bernoulli process of which bears among the 1000 augmented individuals are included in the population. The activity centers (s) were assumed to be uniformly distributed across the habitat, thus we set the prior for the x and y coordinates of s as uniform with the minimum and maximum values of the masked area. The prior for the capture probability at the activity center (p_0) was $\text{Uniform}(0, 1)$. The spatial scale parameter was assumed to be sex-specific so we defined two spatial scale parameters: σ_{female} and σ_{male} . The priors of these parameters were assumed to be $t(\mu = 0, \tau = 0.00055, df = 3)$ truncated at 0. A half normal detection function was used in the model. The likelihood was specified according to the models described in Section 2.2.

Model 3 in Tourani et al. (2020) used the same model specifications as SECR for the individually identified (hair trap) data. For the unidentified detection (camera trap) data, the prior for the detection probability parameter was $\text{Uniform}(0, 1)$. Priors of every other parameter were the same as for the SECR. The likelihood was specified according to the model described in Section 2.3.2.

We used R version 4.1.2 to run all analysis (R Core Team, 2021). The CR M_h model and models from Blanc et al. (2014) were implemented in JAGS and fit via the R package “rjags” (Plummer, 2021) using code provided in Blanc et al. (2014)’s Appendix S1. All other models including the code of model 3 from the supplementary material of Tourani et al. (2020) were executed using the R package “NIMBLE” (de Valpine et al., 2021) with bespoke code provided in the Supporting Information. QGIS version 3.12 (QGIS Development Team, 2022) and R package “sf” (Pebesma, 2018) were used to incorporate the spatial data for the SECR-type models. Package “mcmcplots” was employed to generate the Bayesian diagnostics plots (Curtis, 2018) and “ggplot2” was used for creating density plots (Wickham, 2016).

3.3 | Results

Table 1 provides the summary of grizzly bear detections per method. We used this data to estimate the abundance from the CR model and integrated CR-occupancy models. The results varied, sometimes substantially, among models (Table 2). Most notable are the lower abundance and standard deviations for the integrated CR-O (Blanc) model. (Note that these methods do not provide density estimates unless ad hoc methods are used as spatial data are not considered).

Abundance estimates were much more similar among the spatially explicit models; however, both abundance estimates and estimated standard errors were greater for the integrated camera-DNA SECR models compared with their DNA-only SECR counterparts. To investigate this further, we incorporated a sex covariate into the spatial parameter σ allowing the model to have different home ranges for male versus female bears. Here, again, estimated standard errors were larger for the integrated versus the SECR models (Table 1).

The posterior distributions of N from the CR and integrated CR-O model are shown in Figure 1. The narrow width produced by the integrated model causes estimated standard errors to be much smaller than those from the CR, possibly unrealistically. The posterior distribution of N from integrated SECR model (Figure 2) shows the higher variability associated with the model compared with the standard SECR model.

TABLE 1 Summary of detections from camera traps and hair traps

Detections	Camera trap	Hair trap
Total no. of stations	50	50
Total no. of occasions	8	8
No. of stations with bear detection	38	28
Total no. of detections	143	70
Total no. of individuals detected	N/A	37
Total number of repeat detection of individuals	N/A	19

TABLE 2 Parameter estimates with estimated standard errors in brackets for the six models: Capture-recapture model M_h (CR), model M_h integrated with occupancy from Blanc et al. (2014) (CR-O), SECR, integrated SECR and occupancy from Tourani et al. (2020) Model 3 (SECR-O), SECR with covariate sex on the habitat parameter σ (SECR(sex)), and integrated SECR and occupancy with covariate sex on the habitat parameter (SECR(sex)-O)

Model	N	N_{female}	N_{male}	p_{01}	p_{02}	σ	σ_{female}	σ_{male}
CR	73.36 (31.84)	–	–	–	–	–	–	–
CR-O	40.00 (1.56)	–	–	–	–	–	–	–
SECR	380.28 (87.92)	–	–	0.24 (0.07)	–	7.59 (1.12)	–	–
SECR-O	403.94 (92.76)	–	–	0.19 (0.05)	0.81 (0.14)	8.21 (1.17)	–	–
SECR(sex)	433.31 (105.91)	329.38 (96.38)	103.93 (37.06)	0.26 (0.07)	–	–	5.89 (1.03)	9.50 (2.12)
SECR(sex)-O	497.55 (139.65)	387.61 (130.83)	109.94 (42.88)	0.2 (0.05)	0.82 (0.14)	–	6.32 (1.10)	10.57 (2.41)

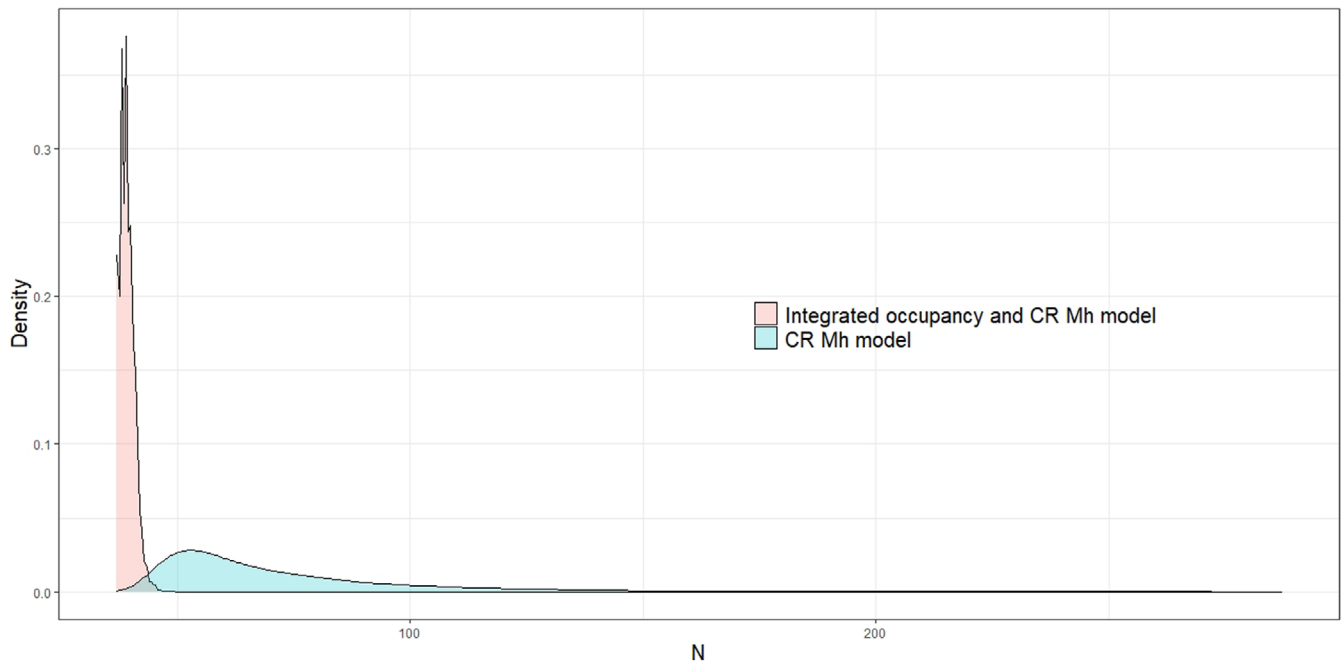


FIGURE 1 Density plots of the posterior distributions of N from the CR and integrated CR-O models of Blanc et al. (2014)

4 | DISCUSSION

Harnessing information from multiple sources of survey data to improve accuracy and precision for abundance estimation is an important development in modern wildlife monitoring and conservation. We studied two such methods that combine camera trap data involving unidentified individuals with identified individuals in hair trap survey data. As is shown in many examples in the literature, the addition of information generally improves parameter estimates, typically by increasing the precision. We see this in Blanc et al. (2014)'s integrated CR model as well as Tourani et al. (2020)'s integrated SECR model. However, for our grizzly bear case study we found this was not the case: both estimated abundance and standard errors are greater in the integrated models. There are several reasons why the integrated models may have reduced precision.

First, one of the assumptions for the integrated models is that data sources are independent. This was not the case for this grizzly bear data as camera traps were at the same location as hair traps. Thus, bears that were captured through hair trapping were highly likely to be captured by the camera traps. The importance of the independence assumption has been described by Schaub and Abadi (2011); however, the assumption of independent data is often overlooked in integrating data sets (see, e.g., for wolves: Horne et al., 2019 and for koalas: Rhodes et al., 2011). Abadi

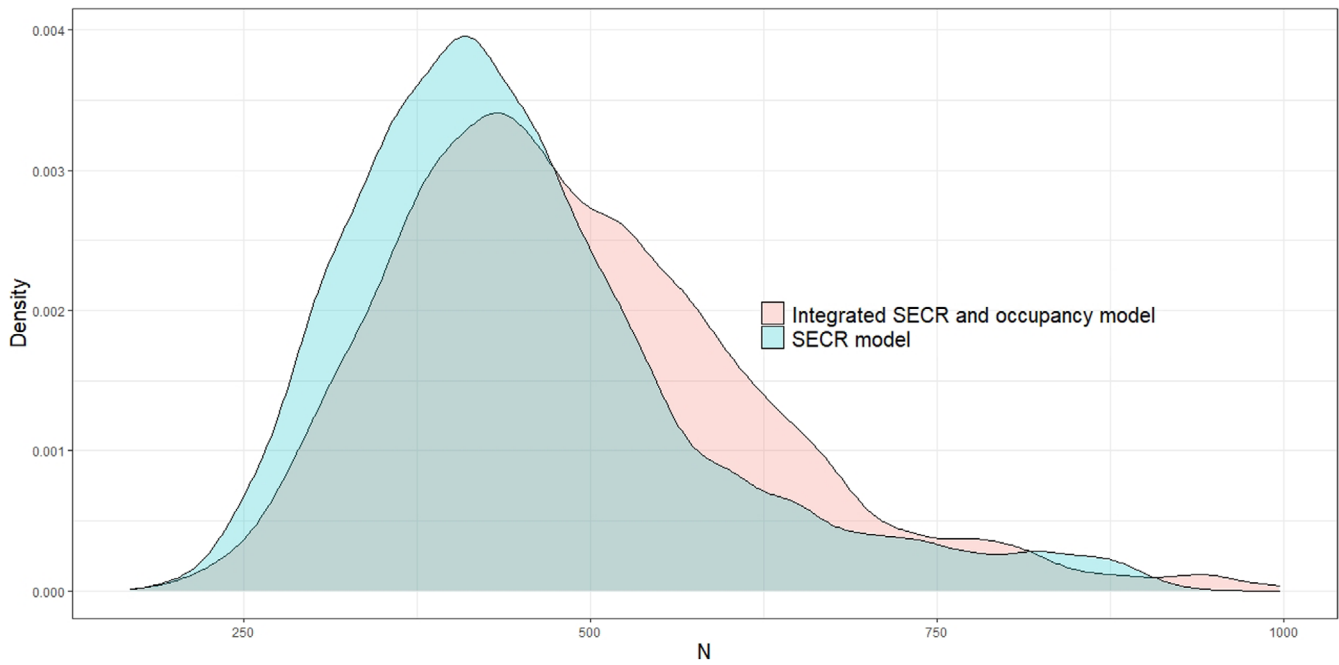


FIGURE 2 Density plots of posterior distributions of N from the SECR and integrated SECR-O models

et al. (2010) explore this assumption for CR, population survey, and reproductive success data concluding that dependent data only slightly affect the accuracy of parameter estimates; however, they found that precision is overestimated when dependent data are combined (the opposite of what we observed). A simulation study to determine the effect of this dependence on parameter estimates would add to this knowledge gap. We are currently developing a model that incorporates this dependence and have planned a future simulation study to determine the effect of dependence on parameter estimates.

Second, it is unclear if these models are robust to model misspecification, which can also affect bias. If there are unknown covariates unaccounted for, this may cause higher variance. To investigate these issues further, we are planning a second simulation study to examine the increased variance and possible bias in the grizzly bear data to determine the influence of the data on bias and precision of the estimators. An increase in variance could also be due to the heterogeneity in not knowing if the same bear or different bears are being captured by the cameras. A future model might make use of the number of detections at the cameras and link the timing of the rub events with some of the camera detections.

It is interesting to note that the abundance/density estimates from the integrated SECR models are higher than SECR models. SECR-based density estimates assume the statistical population—bears detectable by hair traps—represent the biological population. Larger estimates from the integrated models suggest that there may be two statistical populations: one detectable by hair traps, and another not detected by hair traps but detected by camera traps.

Evidence for the two-part population comes from several inferences and a logical deconstruction of the detection process. To be detected by a combined hair/camera trap: (a) a bear must live within the sampling frame during the sampled season, (b) its home range must be proximal to the detector, (c) its movement within that home range must allow for encounter with a detector, and (d) it must be within the detection cone of the passive infra-red sensor of the camera trap (which also includes the hair trap). To be further detected by a hair trap: (a) a bear must engage with the hair trap by rubbing against it, (b) the rub must leave a hair sample with a follicle attached, and (c) the follicle must yield intact DNA not degraded by environmental conditions. Thus, DNA detection is more variable than camera trap detection, as rubbing behavior is not uniform among all bears (Green & Mattson, 2003; Kendall et al., 2019; Lamb et al., 2017; Morehouse et al., 2021). Rubbing behavior varies among age-sex classes and individual behavior, and may be density-dependent. Further, hair samples without attached follicles are quite common (an intermittent tag loss). Finally, when a follicle is captured, the DNA therein degrades over time depending on environmental conditions, especially moisture and heat (Kendall & McKelvey, 2008; von Thaden et al., 2020).

In an empirical comparison of camera versus hair trap detections at rub stations, Fisher et al. (2016) showed that while cameras never failed to capture a bear that left a hair sample, hair detections were always less than camera detections, with the degree of under-sampling varying within a year and among years. At best, monthly site occupancy by a bear was underestimated 50% by hair and at worst, 95%. Therefore integrated models combining camera- and hair-based detection are useful in overcoming failed DNA detections spread heterogeneously throughout the population, as our results suggest. A future model might implement the detection probability of a mixture of bears that tend to rub and bears that do not.

While implementing Blanc et al. (2014)'s integrated model we found that the posterior standard deviation was unusually small and the abundance estimate was nearly equal to the number of observed unique individuals. This is clearly shown in Figure 1 and Table 1 in which abundance is estimated to be 40 and the observed number of unique individuals in the data is 37. This mimicked the results of Blanc et al. (2014) wherein they observed nine unique lynx within their study area and estimated the abundance as 9.96 with [95% CI: 9.00; 13.00], a very narrow range. We believe that this is caused by the fact that the implementation of their model mixes scales relating abundance over the entire area with occupancy at a single site. In the case of the grizzly bears, we know that $N > 37$, suggesting that $\lambda \geq 37$ as well. Substituting this value into Equation (3) would then suggest that Ψ is very close to 1. Moreover, since Ψ is an increasing function of λ , the presence of any apparently unoccupied sites will force N to be as small as possible to accommodate. The model may be applicable if individuals range over the entire study area so that the probability of occupancy at any single site is effectively the same as occupancy of the entire area. However, this is clearly not the case for our grizzly bear example. We are planning on studying this issue more intently through a simulation study and believe that it may be possible to develop models linking occupancy to site abundance rather than population abundance.

With ongoing global biodiversity declines, the need is greater than ever for information on wildlife populations to inform effective conservation decisions. Although wildlife population sampling technology has increased dramatically over the last decade, we conclude that the statistical technology to use this burgeoning body of data has been slower to catch up. The development of integrated models is a substantial step forward but our look “under the hood” shows that further development of the models—especially model components that are highly sensitive to variability in the biology of target animals—is needed to provide robust estimates. Substantially more collaborations between statisticians and ecologists would dramatically increase the rate of improvement of these models.

ACKNOWLEDGMENTS

This work was supported by a CANSSI Collaborative Research Team grant awarded to Simon J. Bonner, Saman Muthukumarana, and Laura L. E. Cowen. Jason T. Fisher was supported by the Oil Sands Monitoring Program; this work does not reflect the position of that program. Data collection was funded by Alberta Innovates-Technology Futures and Alberta Environment and Parks (AEP). Collection was led by Nicole Heim (University of Victoria) and John Paczkowski (AEP) with data processing by Sandra Code (AEP), and data development by Michael Sawaya (Sinopah Wildlife Research Associates) and A. Cole Burton (University of British Columbia).

ORCID

Holly N. Steeves  <https://orcid.org/0000-0001-7553-497X>

Jason T. Fisher  <https://orcid.org/0000-0002-9020-6509>

Simon J. Bonner  <https://orcid.org/0000-0003-2063-4572>

Saman Muthukumarana  <https://orcid.org/0000-0001-8942-5352>

Laura L. E. Cowen  <https://orcid.org/0000-0002-0853-1450>

REFERENCES

- Abadi, F., Gimenez, O., Arlettaz, R., & Schaub, M. (2010). An assessment of integrated population models: Bias, accuracy, and violation of the assumption of independence. *Ecology*, 91(1), 7–14. <https://doi.org/10.1890/08-2235.1>
- Balkenhol, N., Cushman, S., Storfer, A., & Waits, L. (2015). *Landscape genetics: Concepts, methods, applications*. John Wiley & Sons. <https://doi.org/10.1002/9781118525258.ch01>
- Besbeas, P., Freeman, S., & Morgan, B. (2005). The potential of integrated population modelling. *Australian and New Zealand Journal of Statistics*, 47, 35–48. <https://doi.org/10.1111/j.1467-842X.2005.00370.x>
- Besbeas, P., Freeman, S., Morgan, B., & Catchpole, E. (2002). Integrating mark-recapture-recovery and census data to estimate animal abundance and demographic parameters. *Biometrics*, 58, 1–16. <https://doi.org/10.1111/j.0006-341X.2002.00540.x>

- Blanc, L., Marboutin, E., Gatti, S., Zimmermann, F., & Gimenez, O. (2014). Improving abundance estimation by combining capture–Recapture and occupancy data: Example with a large carnivore. *Journal of Applied Ecology*, 51(6), 1733–1739. <https://doi.org/10.1111/13652664.12319>
- Borchers, D. L., & Efford, M. G. (2008). Spatially explicit maximum likelihood methods for capture–Recapture studies. *Biometrics*, 64(2), 377–385. <https://doi.org/10.1111/j.1541-0420.2007.00927.x>
- Buckland, S. T., Anderson, D. R., Burnham, K. P., Laake, J. L., Borchers, D. L., & Thomas, L. (2001). *Introduction to distance sampling: Estimating abundance of biological populations*. Oxford University Press. <https://doi.org/10.2307/2532812>
- Burgar, J., Stewart, F. E., Volpe, J. P., Fisher, J. T., & Burton, A. C. (2018). Estimating density for species conservation: Comparing camera trap spatial count models to genetic spatial capture-recapture models. *Global Ecology and Conservation*, 15, e00411. <https://doi.org/10.1016/j.gecco.2018.e00411>
- Campbell, L. A., Long, R. A., & Zielinski, W. J. (2008). *Integrating multiple methods to achieve survey objectives*. In R. A. Long, P. Mackay, W. J. Zielinski, & J. C. Ray (Eds.), *Noninvasive Survey Methods for Carnivores* (pp. 223–237). Island Press.
- Chao, A. (1987). Estimating the population size for capture-recapture data with unequal catchability. *Biometrics*, 43(4), 783–791. <https://doi.org/10.2307/2531532>
- Curtis, S. M. (2018). mcmcplots: Create plots from MCMC output. *R package version 0.4.3*. <https://CRAN.R-project.org/package=mcmcplots>
- Davis, A. J., McCreary, R., Psiropoulos, J., Brennan, G., Cox, T., Partin, A., & Pepin, K. M. (2018). Quantifying site-level usage and certainty of absence for an invasive species through occupancy analysis of camera-trap data. *Biological Invasions*, 20(4), 877–890. <https://doi.org/10.1007/s10530-017-1579-x>
- de Valpine, P., Paciorek, C., Turek, D., Michaud, N., Anderson-Bergman, C., Obermeyer, F., Wehrhahn-Cortes, C., Rodriguez, A., Temple-Lang, D., & Paganin, S. (2021). NIMBLE user manual. *R package manual version 0.12.1*. <https://doi.org/10.5281/zenodo.1211190>
- Devarajan, K., Morelli, T. L., & Tenan, S. (2020). Multi-species occupancy models: Review, roadmap, and recommendations. *Ecography*, 43(11), 1612–1624. <https://doi.org/10.1111/ecog.04957>
- Efford, M. (2019). Habitat masks in the package secr. <https://www.otago.ac.nz/density/pdfs/secrhabitatmasks.pdf> Accessed: 11 March 2022
- Efford, M. G. (2004). Density estimation in live-trapping studies. *Oikos*, 106(3), 598–610. <https://doi.org/10.1111/j.0030-1299.2004.13043.x>
- Efford, M. G., Borchers, D. L., & Byrom, A. E. (2009). *Density estimation by spatially explicit capture–recapture: Likelihood-based methods*. In *Modeling demographic processes in marked populations. Volume 3 of Environmental and Ecological Statistics* (pp. 255–269). Springer. <https://doi.org/10.1007/978-0-387-78151-811>
- Efford, M. G., & Hunter, C. M. (2018). Spatial capture–Mark–Resight estimation of animal population density. *Biometrics*, 74(2), 411–420. <https://doi.org/10.1111/biom.12766>
- Fisher, J. T., & Bradbury, S. (2014). A multi-method hierarchical modeling approach to quantifying bias in occupancy from noninvasive genetic tagging studies. *The Journal of Wildlife Management*, 78(6), 1087–1095. <https://doi.org/10.1002/jwmg.750>
- Fisher, J. T., Heim, N., Code, S., & Paczkowski, J. (2016). Grizzly bear noninvasive genetic tagging surveys: Estimating the magnitude of missed detections. *PLoS One*, 11(9), e0161055. <https://doi.org/10.1371/journal.pone.0161055>
- Foster, R. J., & Harmsen, B. J. (2012). A critique of density estimation from camera-trap data. *The Journal of Wildlife Management*, 76(2), 224–236. <https://doi.org/10.1002/jwmg.275>
- Gibbs, J. P. (2000). *Monitoring populations*. In L. Boitani & T. K. Fuller (Eds.), *Research techniques in animal ecology* (pp. 213–252). Columbia University Press.
- Green, G. I., & Mattson, D. J. (2003). Tree rubbing by yellowstone grizzly bears *Ursus arctos*. *Wildlife Biology*, 9, 1–9. <https://doi.org/10.2981/wlb.2003.002>
- Greenberg, S., Godin, T., & Whittington, J. (2019). Design patterns for wildlife-related camera trap image analysis. *Ecology and Evolution*, 9(24), 13706–13730. <https://doi.org/10.1002/ece3.5767>
- Horne, J. S., Ausband, D. E., Hurley, M. A., Struthers, J., Berg, J. E., & Groth, K. (2019). Integrated population model to improve knowledge and management of Idaho wolves. *The Journal of Wildlife Management*, 83(1), 32–42.
- Huettmann, F. (2005). Databases and science-based management in the context of wildlife and habitat: Toward a certified iso standard for objective decision-making for the global community by using the internet. *Journal of Wildlife Management*, 69(2), 466–472. [https://doi.org/10.2193/0022-541X\(2005\)069\[0466:DASMIT\]2.0.CO;2](https://doi.org/10.2193/0022-541X(2005)069[0466:DASMIT]2.0.CO;2)
- Karanth, K. U. (1995). Estimating tiger *Panthera Tigris* populations from camera-trap data using capture-recapture models. *Biological Conservation*, 71(3), 333–338. [https://doi.org/10.1016/0006-3207\(94\)00057-W](https://doi.org/10.1016/0006-3207(94)00057-W)
- Kendall, K. C., Graves, T. A., Royle, J. A., Macleod, A. C., McKelvey, K. S., Boulanger, J., & Waller, J. S. (2019). Using bear rub data and spatial capture-recapture models to estimate trend in a brown bear population. *Scientific Reports*, 9, 1–11. <https://doi.org/10.1038/s41598-019-52783-5>
- Kendall, K. C., & McKelvey, K. S. (2008). Hair collection. *Noninvasive Survey Methods for Carnivores*, 106, 141–182.
- Lamb, C. T., Mowat, G., Gilbert, S. L., McLellan, B. N., Nielsen, S. E., & Boutin, S. (2017). Density-dependent signaling: An alternative hypothesis on the function of chemical signaling in a non-territorial solitary carnivore. *PLoS One*, 12, e0184176. <https://doi.org/10.1371/journal.pone.0184176>
- Lebreton, J.-D., Burnham, K. P., Clobert, J., & Anderson, D. R. (1992). Modelling survival and testing biological hypotheses using marked animals: A unified approach with case studies. *Ecological Monographs*, 62, 67–118. Discusses most of capture-recapture theory. Mentions models using logistic regression for open populations.
- MacKenzie, D., Nichols, J., Royle, J. A., Pollock, K., Bailey, L., & Hines, J. (2017). *Occupancy estimation and modeling* (2nd ed.). Academic Press.

- MacKenzie, D. I., Nichols, J. D., Lachman, G. B., Droege, S., Royle, J. A., & Langtimm, C. A. (2002). Estimating site occupancy rates when detection probabilities are less than one. *Ecology*, 83(8), 2248–2255. [https://doi.org/10.1890/0012-9658\(2002\)083\[2248:ESORWD\]2.0.CO;2](https://doi.org/10.1890/0012-9658(2002)083[2248:ESORWD]2.0.CO;2)
- Magoun, A. J., Long, C. D., Schwartz, M. K., Pilgrim, K. L., Lowell, R. E., & Valkenburg, P. (2011). Integrating motion-detection cameras and hair snags for wolverine identification. *The Journal of Wildlife Management*, 75(3), 731–739. <https://doi.org/10.1002/jwmg.107>
- Morehouse, A. T., Loosen, A. E., Graves, T. A., & Boyce, M. S. (2021). The smell of success: Reproductive success related to rub behavior in brown bears. *PLoS One*, 16, e0247964. <https://doi.org/10.1371/journal.pone.0247964>
- Otis, D. L., Burnham, K. P., White, G. C., & Anderson, D. R. (1978). Statistical inference from capture data on closed animal populations. *Wildlife Monographs*, 62, 3–135.
- Paetkau, D. (2003). An empirical exploration of data quality in DNA-based population inventories. *Molecular Ecology*, 12(6), 1375–1387. <https://doi.org/10.1046/j.1365-294X.2003.01820.x>
- Paetkau, D., Calvert, W., Stirling, I., & Strobeck, C. (1995). Microsatellite analysis of population structure in Canadian polar bears. *Molecular Ecology*, 4(3), 347–354. <https://doi.org/10.1111/j.1365-294X.1995.tb00227.x>
- Palencia, P., Vicente, J., Barroso, P., Barasona, J., Soriguer, R. C., & Acevedo, P. (2019). Estimating day range from camera-trap data: The animals' behaviour as a key parameter. *Journal of Zoology*, 309(3), 182–190. <https://doi.org/10.1111/jzo.12710>
- Pebesma, E. (2018). Simple features for R: Standardized support for spatial vector data. *The R Journal*, 10(1), 439–446. <https://doi.org/10.32614/RJ-2018-009>
- Plummer, M. (2021). *rjags: Bayesian graphical models using MCMC*. R package version 4-12. <https://CRAN.R-project.org/package=rjags>
- Pollock, K. H. (2000). Capture-recapture models. *Journal of the American Statistical Association*, 95(449), 293–296.
- QGIS Development Team. (2022). *QGIS geographic information system*. QGIS Association. <https://www.qgis.org>
- R Core Team. (2021). *R: A language and environment for statistical computing*. R Foundation for Statistical Computing. <https://www.R-project.org/>
- Rhodes, J. R., Ng, C. F., de Villiers, D. L., Preece, H. J., McAlpine, C. A., & Possingham, H. P. (2011). Using integrated population modelling to quantify the implications of multiple threatening processes for a rapidly declining population. *Biological Conservation*, 144(3), 1081–1088.
- Rich, L. N., Kelly, M. J., Sollmann, R., Noss, A. J., Maffei, L., Arispe, R. L., Paviolo, A., De Angelo, C. D., Di Blanco, Y. E., & Di Bitetti, M. S. (2014). Comparing capture-recapture, mark-resight, and spatial mark-resight models for estimating puma densities via camera traps. *Journal of Mammalogy*, 95(2), 382–391. <https://doi.org/10.1644/13-MAMM-A-126>
- Royle, J. A., Dorazio, R. M., & Link, W. A. (2007). Analysis of multinomial models with unknown index using data augmentation. *Journal of Computational and Graphical Statistics*, 16(1), 67–85. <https://doi.org/10.1198/106186007X181425>
- Royle, J. A., Karanth, K. U., Gopalaswamy, A. M., & Kuman, N. S. (2009). Bayesian inference in camera trapping studies for a class of spatial capture-recapture models. *Ecology*, 90, 3233–3244. <https://doi.org/10.1890/08-1481.1>
- Royle, J. A., & Nichols, J. D. (2003). Estimating abundance from repeated presence–Absence data or point counts. *Ecology*, 84(3), 777–790. [https://doi.org/10.1890/0012-9658\(2003\)084\[0777:EAFRPA\]2.0.CO;2](https://doi.org/10.1890/0012-9658(2003)084[0777:EAFRPA]2.0.CO;2)
- Royle, J. A., & Young, K. V. (2008). A hierarchical model for spatial capture–Recapture data. *Ecology*, 89(8), 2281–2289.
- Schaub, M., & Abadi, F. (2011). Integrated population models: A novel analysis framework for deeper insights into population dynamics. *Journal of Ornithology*, 152(Suppl 1), 227–237. <https://doi.org/10.1007/s10336-010-0632-7>
- Schofield, M. R., & Barker, R. J. (2011). Full open population capture–Recapture models with individual covariates. *Journal of Agricultural, Biological, and Environmental Statistics*, 16, 253–268. <https://doi.org/10.1007/s13253-010-0052-4>
- Schofield, M. R., & Barker, R. J. (2014). Hierarchical modeling of abundance in closed population capture–Recapture models under heterogeneity. *Environmental and Ecological Statistics*, 21(3), 435–451. <https://doi.org/10.1007/s10651-013-0262-3>
- Schwarz, C. J., & Arnason, A. N. (1996). A general methodology for the analysis of capture-recapture experiments in open populations. *Biometrics*, 52, 860–873. <http://www.jstor.org/stable/2533048>
- Seber, G. (2002). *The estimation of animal abundance and related parameters*. Blackburn Press.
- Sollmann, R. (2018). A gentle introduction to camera-trap data analysis. *African Journal of Ecology*, 56, 740–749. <https://doi.org/10.1111/aje.12557>
- Sollmann, R., Gardner, B., Parsons, A. W., Stocking, J. J., McClintock, B. T., Simons, T. R., Pollock, K. H., & O'Connell, A. F. (2013). A spatial mark–Resight model augmented with telemetry data. *Ecology*, 94(3), 553–559. <https://doi.org/10.1890/12-1256.1>
- Tourani, M., Dupont, P., Nawaz, M. A., & Bischof, R. (2020). Multiple observation processes in spatial capture–Recapture models: How much do we gain? *Ecology*, 101(7), e03030. <https://doi.org/10.1002/ecy.3030>
- von Thaden, A., Nowak, C., Tiesmeyer, A., Reiners, T. E., Alves, P. C., Lyons, L. A., Mattucci, F., Randi, E., Cragolini, M., & Galián, J. (2020). Applying genomic data in wildlife monitoring: Development guidelines for genotyping degraded samples with reduced single nucleotide polymorphism panels. *Molecular Ecology Resources*, 20, 662–680. <https://doi.org/10.1111/1755-0998.13136>
- White, G. C. (2001). Why take calculus? Rigor in wildlife management. *Wildlife Society Bulletin*, 29(1), 380–386.
- Whittington, J., Hebblewhite, M., & Chandler, R. B. (2018). Generalized spatial mark–Resight models with an application to grizzly bears. *Journal of Applied Ecology*, 55(1), 157–168. <https://doi.org/10.1111/1365-2664.12954>
- Wickham, H. (2016). *ggplot2: Elegant graphics for data analysis*. Springer-Verlag <https://ggplot2.tidyverse.org>
- Witmer, G. W. (2005). Wildlife population monitoring: Some practical considerations. *Wildlife Research*, 32(3), 259–263. <https://doi.org/10.1071/WR04003>

- Yoccoz, N. G., Nichols, J. D., & Boulmier, T. (2001). Monitoring of biological diversity in space and time. *Trends in Ecology and Evolution*, 16(8), 446–453. [https://doi.org/10.1016/S0169-5347\(01\)02205-4](https://doi.org/10.1016/S0169-5347(01)02205-4)
- Zipkin, E. F., & Saunders, S. P. (2018). Synthesizing multiple data types for biological conservation using integrated population models. *Biological Conservation*, 217, 240–250. <https://doi.org/10.1016/j.biocon.2017.10.017>

SUPPORTING INFORMATION

Additional supporting information can be found online in the Supporting Information section at the end of this article.

How to cite this article: Jahid, M., Steeves, H. N., Fisher, J. T., Bonner, S. J., Muthukumarana, S., & Cowen, L. L. E. (2022). Shooting for abundance: Comparing integrated multi-sampling models for camera trap and hair trap data. *Environmetrics*, e2761. <https://doi.org/10.1002/env.2761>